

Liquid Flow Behaviour of Bubble Columns

By Yuji SANO* and Kazuyoshi YAMAMOTO*

(Received July 31, 1974)

Abstract

Liquid flow behaviour of a bubble column was investigated experimentally with emphasis on its turbulent motion. Pictures of tracer particles suspended in liquid were photographed with a high speed cinecamera on colour films avoiding the confusion of images of particles and bubbles. Trajectory of particles on the films were followed by a film analyzer and fluctuating velocities of tracers (as liquid) were obtained. Liquid flow behaviour was then analyzed statistically for the terms of the mean liquid velocity distribution, the fluctuating velocity distribution, the autocorrelation curve, the turbulent scale and so on.

- 1) Liquid flow in a bubble column showed the upward flow in the core with violent eddy motion and downward flow near the wall. The radial distribution of axial mean liquid flow velocity was consistent with Miyauchi's model¹⁾ and the radial mean velocity was nearly equal to zero.
- 2) Liquid velocity fluctuates greatly in a short time as indicated by the intensity of turbulence of axial liquid velocity which was about 90% at the center.
- 3) The eddy scale in the center was about 1/6th-1/7th of column diameter in radial direction and about one half in axial direction.
- 4) In the down flow region near the wall, a large fluctuation with a characteristic periodicity was observed in the periodogram.
- 5) The liquid flow behaviour was not much influenced by liquid viscosity 1-12 c. p.

Introduction

Bubble columns are widely used as gas-liquid contacting apparatus in gas absorption, gas-liquid reaction, and catalytic reaction. However, the liquid flow behaviour in the bubble flow regime, usually used as operating condition in bubble columns, is not well known. The liquid flow behaviour is an important problem connected with the basic factors of bubble column design, such as mass transfer between gas and liquid, heat conduction on the wall, and liquid mixing. Although many investigations of liquid behaviour have been tried, enough information has not been obtained because of the difficulty of measurement due to the existence of bubbles in liquid. Yoshitome et al²⁾ confirmed the liquid flow pattern by measuring the drag force of a spherical float installed in a bubble column. Miyauchi et al¹⁾ obtained the distribution of mean liquid velocity and gas hold-up by the isokinetic sampling method. He compared the mean liquid velocity, which is rather scattered, with the theoretical results derived from his fluid circulation model. Koide et al³⁾ reported the distribution of \bar{V}_z obtained with the impact tube. However, these reports of liquid flow data in a bubble column are restricted to only average values and the turbulent behaviour of liquid caused by rising bubbles

* Department of Chemical Engineering

is still unknown. Recently Kojima et al⁴⁾ tried to measure the fluctuating liquid velocity by the use of a hot film anemometer. They obtained an one dimensional energy spectrum and some information on turbulent liquid flow in a bubble column.

This report covers an investigation into the liquid flow behaviour in a bubble column. Turbulent liquid motion was recorded on cinefilm which provided the trajectory of tracer particles suspended in the liquid of a bubble column for analysis.

Apparatus and Analysis Procedure

The experimental apparatus is shown schematically in Fig. 1. The column, 100 mm inside diameter and 120 cm in height, made of transparent acrylic resin was equipped with a jacket for the purpose of both avoiding distortion of light when pictures

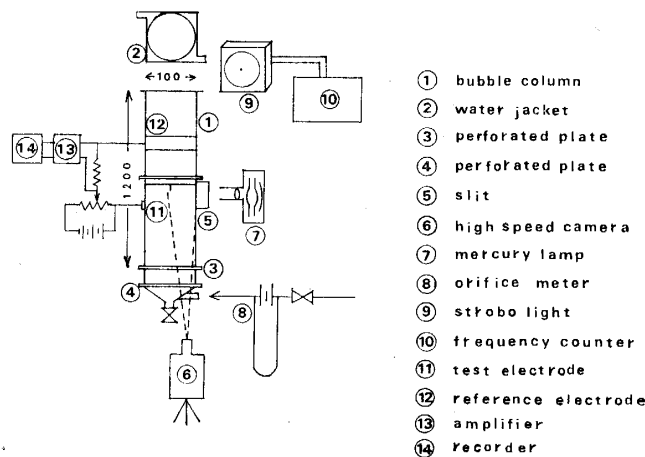


Fig. 1 Experimental apparatus.

were taken and keeping the liquid temperature constant. The gas distributor had nineteen holes of 0.5 mm diameter, perforated with the distance 20 mm in a regular triangular manner. About 3 g polyethylene particles colored with orange fluorescent pigment and adjusted to the density of water (diameter; 400 μ , density; 1.03 g/cm³) were suspended as tracers into deionized water of 8 l. The pictures were taken by a high-speed cinecamera (HITACHI-16H) with 100 feet of color film at the position, 55 cm above the gas distributor, where the parallel light of a mercury lamp came through a slit of 2 mm in width. The flash of a strobo light, connected to a frequency counter, produced bright lines at intervals on the film providing a film speed check. To obtain the magnification ratio on film, a scale was placed in the column. The average gas hold-up, i.e. the average gas volumetric fraction, was measured according to the liquid height elevation*). Gas was air introduced from a compressor and its flow rate was measured by an orifice flowmeter. Liquids were both deionized water and C. M. C**)-water

*) gas hold-up ϵ ; $\epsilon = (L - L_0)/L$. where L ; liquid height with gas input, L_0 ; liquid height without gas input.

***) carboxyl methyl cellulose.

solution (12.6 c.p) which was also used in order to know the influence of liquid viscosity. Experimental conditions and fluid properties are shown in Table 1. The gas input was kept constant, which was presented with the term of superficial velocity***) $U_g = 1.0$ cm/sec.

Table 1 Experimental conditions and liquid properties.

		Water	C.M.C. solution
Liquid viscosity	(c.p.)	0.8	12.6
Superficial gas velocity	(cm/sec)	1.08	1.02
Average gas hold-up	(%)	4.1	3.5
Liquid temperature	(°C)	30	22
Total sampling time on film	(sec)	9.3	16.8
Average frame time interval on film	(sec)	2.6×10^{-3}	4.8×10^{-3}

Diffusion coefficient of ferri cyanide ion in water at 20°C : 6.83×10^{-6} (cm²/sec)

Pictures were projected about three times larger than actual size on the screen of a film analyzer (Filmotion; Bell & Howell). Several sampling zones were set up on a glass projection screen in a radial direction in order to measure the radial distribution of liquid velocity. Selective particle images within the sampling zone (actual size of the flow field; 2–4 mm in width and 3–10 mm in height) were continuously followed with the accuracy of 10^{-2} mm on a film and their coordinates were recorded on each picture frame. Coordinate difference between two successive frames give the axial and radial displacement in the time lapse per frame. If the particles move the distance Δr for radial and Δz for axial in the time of a frame interval, Δt , the radial and axial velocities are

$$V_z = \frac{\Delta z}{\Delta t}, \quad V_r = \frac{\Delta r}{\Delta t} \quad \dots\dots\dots(1)$$

The instantaneous axial and radial liquid velocities within a sampling zone can be obtained from Eq. (1). The liquid velocity variations with time were obtained by the analysis of successive pictures on film.

The mean liquid velocity can be obtained by averaging velocity data.

$$\bar{V}_z = \frac{1}{N} \sum_{i=1}^N V_{zi}, \quad \bar{V}_r = \frac{1}{N} \sum_{i=1}^N V_{ri} \quad \dots\dots\dots(2)$$

The average value of the square of fluctuating velocities and Reynolds shearing stress can be obtained from Eq. (3) and (4) because the time average of fluctuating velocities is zero.

$$\overline{v_z^2} = (\overline{\bar{V}_z + v_z})^2 - \bar{V}_z^2, \quad \overline{v_r^2} = (\overline{\bar{V}_r + v_r})^2 - \bar{V}_r^2 \quad \dots\dots\dots(3)$$

$$\overline{v_r v_z} = (\overline{\bar{V}_r + v_r})(\overline{\bar{V}_z + v_z}) - \bar{V}_r \bar{V}_z \quad \dots\dots\dots(4)$$

***) U_g = volumetric gas flow rate/cross sectional area of column.

in which the values of \bar{V}_z and \bar{V}_r can be obtained from Eq. (2).

The autocorrelation function for liquid motion can be obtained by averaging the product of pairs of fluctuating velocities, $v_z(t)$, at a certain time t and $v_z(t+\tau)$ at a later time, $t+\tau$. The delay time changed between zero and a few seconds. This calculation was provided by a digital computer in a discrete form.

$$C_{zz}(\tau') = \frac{1}{N-\tau'} \sum_{i=1}^{N-\tau'} v_z(t') v_z(t'+\tau'), \quad \tau' = 0, 1, \dots, h \quad \dots\dots\dots(5)$$

$$\tau' = \tau / \Delta t. \quad t' = t / \Delta t$$

in which N is the total number of data. A Fourier cosine transformation of the autocorrelation function, i.e. energy spectrum or periodogram, is given in Eq. (6) in a discrete form.

$$E(f) = \Delta t \left\{ C_{zz}(0) + 2 \sum_{\tau'=1}^{h-1} \cos(2\pi \frac{r}{2h} \tau') C_{zz}(\tau') + (-1)^r C_{zz}(h) \right\} \quad \dots\dots\dots(6)$$

$$f = \frac{r}{2h\Delta t} \quad r = 0, 1, \dots, h$$

in which f means frequency and h means the data number of maximum delay time of the autocorrelation function. Usually a smoothed energy spectrum is obtained by averaging $E(f)$ over frequencies in the neighborhood of f , as dictated by the shape of the weight function, i.e. the spectral window. In this analysis, the procedure of Akaike⁵⁾ was used as a spectral window.

The specific correlation coefficient of two liquid velocities at the distance, r , can be obtained in Eq. (7).

$$C'_{zz}(r) = \frac{1}{N} \frac{\sum_{i=1}^N v_i(x) v_i(x+r)}{\sqrt{v(x)^2} \cdot \sqrt{v(x+r)^2}} \quad \dots\dots\dots(7)$$

The liquid velocity distribution in the boundary layer near the wall can not be obtained by the preceding tracer technique. Therefore, we measured the velocity gradient at the wall using the technique developed by Hanratty et al⁶⁾. According to his method, the instantaneous diffusion limited current can be measured for the electrochemical reaction $(\text{Fe}(\text{CN})^{-3} + e \rightarrow \text{Fe}(\text{CN})^{-4})$ on a small circular electrode and the wall shearing stress can be obtained from following equations.

$$K = \frac{I}{AF(C_b - C_w)} \quad \text{where } C_w = 0 \quad \dots\dots\dots(8)$$

$$\bar{K} = \frac{3}{2\Gamma(4/3)(9)^{1/3}} \left(\frac{DS_x}{L_e} \right)^{1/3} \quad \dots\dots\dots(9)$$

$$\tau_w = -\mu \frac{S_x}{g_c} \quad \dots\dots\dots(10)$$

In this experiment, the copper electrode (diameter; 0.054 cm) was used as mass transfer rate measuring electrode (cathode). Potential difference between cathode and anode was 0.65 V, which ensures that the diffusion of ferri-cyanide ion to the electrode surface controls the whole transport process. The 8 l solution which contained 0.005 mol/l of both potassium ferricyanide and potassium ferrocyanide and 0.1 N sodium chloride, was used at 20°C for wall velocity gradient measurement. In this experiment, nitrogen gas was used instead of air in order to avoid the effect of oxidation reaction. The effects of ions and N₂ gas on liquid flow behaviour were assumed to be negligible.

Results and Discussion

The film used for the calculation of liquid velocity was about 3500 frames which correspond to times of 9.3 sec for water and 16.8 sec for C.M.C-water solution. For C.M.C-water solution, the film speed of the cinecamera was reduced on account of lower liquid velocity. The start up portions of the film were omitted from analyzation, since the high-speed cinecamera starts with low speed and needs a short time to reach the setting speed. Velocity data was calculated from Eq. (1). The data from series of 20 successive frames were averaged and these average velocities were used as instantaneous velocities for the middle value of the frame time. Because the individual frame data were considered to involve about 15% error due to the reading error of coordinates on the projected plane of the film analyzer. Fig. 2 shows the water velocity fluctuation with time lapse for several radial positions. Even in the center of the column the upward flow predominant region, sometimes downward flow was observed ((A) shown in Fig. (2)) and near the wall, the downward flow region sometimes showed upward flow ((B) shown in Fig. (2)). In such a violent fluctuation, the first problem is to determine how much time lapse is enough to obtain the average value. In Fig. 3, the average values for sampling time t were plotted with time t on the value of mean axial velocities and the r.m.s. of fluctuating velocities. It is mentioned that the time mean values for \bar{V}_z and $\sqrt{\bar{v}_z^2}$ show large variation for small time t but begin to converge to certain constant values for about $t=7$ sec. The sampling time of 9.3 sec for water would be allowable time length to obtain a reasonable average value.

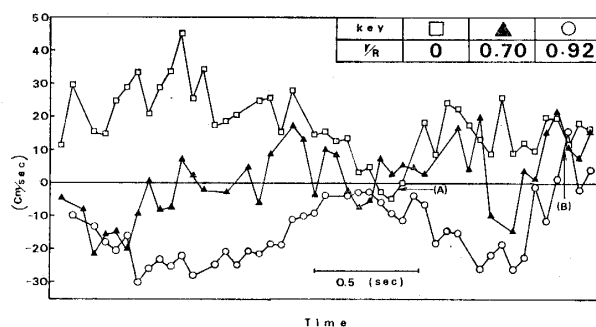


Fig. 2 Fluctuations of V_z .

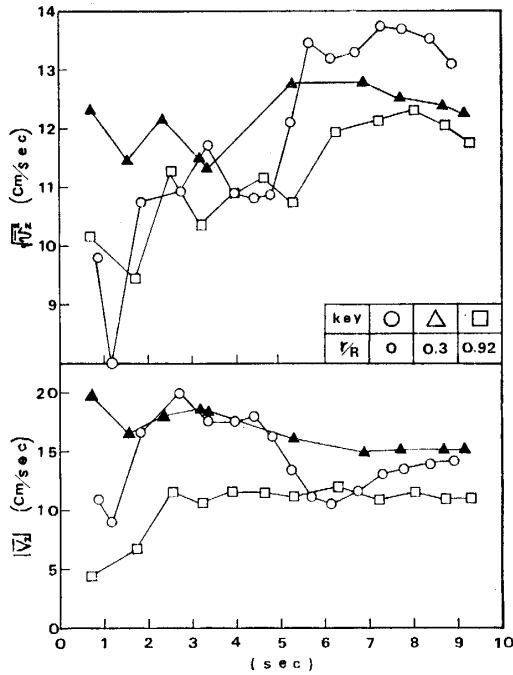


Fig. 3 Variation of average value with sampling time.

1) Radial distribution of time average axial and radial velocities

The average velocities calculated from Eq. (2) for both radial and axial were plotted with dimensionless radial distance $\phi = r/R$ in Fig. 4 for water at room temperature. There was an upward flow induced by air bubbles in the core part. The axial velocity showed the maximum at the center, decreased with radial distance and fell to zero at the position of $\phi = 0.72$. For $\phi > 0.72$, water flowed downwards and downward velocity increased for ϕ . At the wall surface, the velocity might become zero but our observation could not detect the velocity distribution in the boundary layer near the wall. The

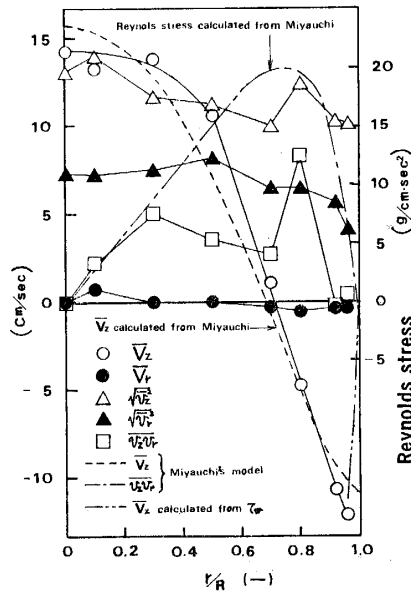


Fig. 4 Radial distribution of mean values for water.

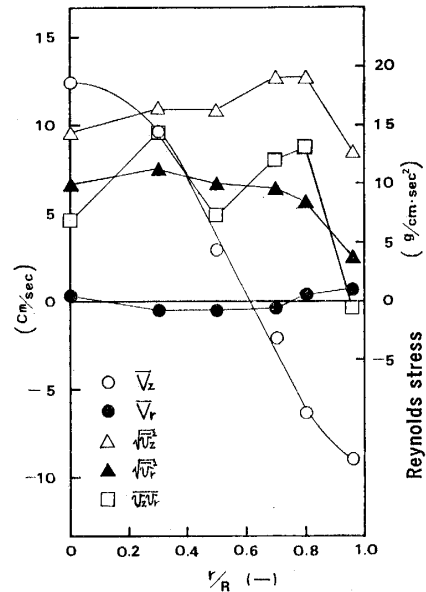


Fig. 5 Radial distribution of mean values for C.M.C.-water solution.

radial velocities were almost zero for the whole range of the radius as shown in Fig. 4. Fig. 5 shows also the distribution of liquid velocities for C. M. C.-water solution. The features of distribution were almost the same as for water, but the zero velocity point was located somewhat closer to center than that for water.

Miyauchi et al¹⁾ derived the axial velocity distribution equations for bubble columns assuming one dimensional flow with constant eddy diffusivity for turbulent core and the hypothetical boundary condition of slip velocity \bar{V}_{zw} at the wall. They also gave the empirical equations of eddy diffusivity and gas hold-up distribution.

$$\bar{V}_z = \bar{V}_{zw}[\Gamma_1(1 - \phi^2) - 1] + \frac{\rho g R^2}{\mu_t} [I(\phi) - (1 - \phi^2)\Gamma_0] \quad \dots\dots\dots(11)$$

where

$$\Gamma_1 = \frac{\int_0^1 \phi [1 - f(\phi)] d\phi}{\int_0^1 [1 - f(\phi)] (1 - \phi^2) \phi d\phi} \quad \dots\dots\dots(12)$$

$$\Gamma_0 = \frac{\int_0^1 [1 - f(\phi)] \phi d\phi \int_\phi^1 \frac{d\phi}{\phi} \int_0^\phi \phi f(\phi) d\phi}{\int_0^1 [1 - f(\phi)] [1 - \phi^2] \phi d\phi} \quad \dots\dots\dots(13)$$

$$I(\phi) = \int_\phi^1 \frac{d\phi}{\phi} \int_0^\phi \phi f(\phi) d\phi \quad \dots\dots\dots(14)$$

$$\bar{V}_{zw} = \frac{134.6 \mu_t \Gamma_1}{\rho R} \left[-1 + \sqrt{1 + \frac{R^3 \rho^2 g (2\Gamma_0 - I(1))}{134.6 (\mu_t \Gamma_1)^2}} \right] \quad \dots\dots\dots(15)$$

$$\mu_t = 0.05 D_T^{1.8} \quad \dots\dots\dots(16)$$

$$\varepsilon = \varepsilon_0 (1 - \phi^8) \quad \dots\dots\dots(17)$$

It is interesting that the eddy diffusivity does not depend on viscosity in Eq. (16). The calculated curves of axial velocity distribution using these equations were also plotted in Fig. 4 and 5. These curves were almost consistent with our experimental results in the turbulent core. The boundary flow near the wall can not be presented in Miyauchi's equations. The possible approach of velocity distribution for boundary flow will be given by the relation of u^+ vs. y^+ for the homogeneous pipe flow. Fig. 6 shows the relation of superficial gas velocity vs. the wall shearing stress measured for the potassium ferri and ferro cyanede-water solution. The wall shearing stress for the conditions of Fig. 4 ($u_g = 1.08$ cm/sec) were $\tau_w = 0.82$ (dyne/cm²). The variation of gas hold-up with gas superficial velocity are also shown in Fig. 6.

The velocity distribution near the wall is assumed as boundary layer equations of pipe flow.

$$u^+ = y^+ \quad \text{for } y^+ < 5 \quad \dots\dots\dots(18)$$

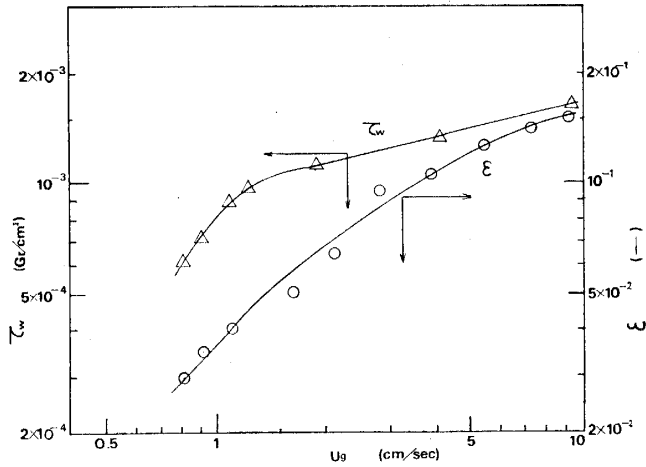


Fig. 6 The effect of superficial gas velocity on shearing stress and gas hold-up.

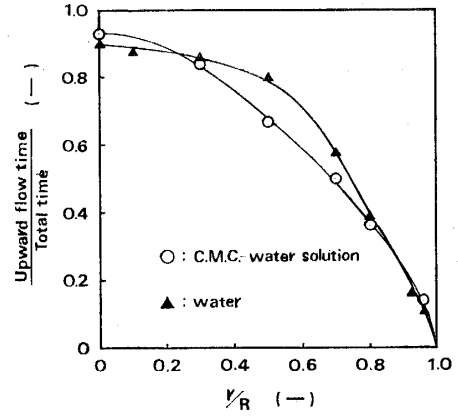


Fig. 7 Radial variation of upward flow time ratio.

$$v^+ = -3.05 + 5.0 \ln y^+ \quad \text{for } 5 < y^+ < 30 \quad \dots\dots\dots(19)$$

The value of \bar{V}_z calculated from Eq. (19) and τ_w were coincident with the value of experimental data at $y = 2.0 \text{ mm}$ ($y^+ = 22$). The average velocity distributions were checked with the mass balance equation.

$$\int_0^R r \rho [1 - f(\phi)] \bar{V}_z dr = 0 \quad \dots\dots\dots(20)$$

assuming the one dimensional flow with zero axial gradient of $d\bar{V}_z/dz$. $f(\phi)$ were assumed, $\epsilon_0(1 - \phi^8)$, according to Miyauchi's results¹⁾. In Fig. 4 for water, the downward volume rate of flow exceeded by 18% that of upward flow. And in Fig. 5 for 12.6 c.p C.M.C. solution the excess rate of down flow was about 50%. These errors were perhaps due to the error of upward flow velocity. Greater velocities of particles on the rear of bubbles might not be measured which perhaps contributed to the error of upward flow velocity measurement.

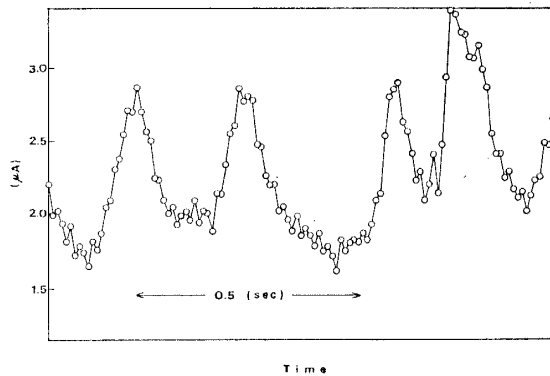
2) Fluctuating behaviour of the flow

One of the characteristics for turbulent flow was r.m.s. of fluctuating velocity or intensity of turbulence. These values have not been reported for bubble columns. Fluctuating velocities were presented in r.m.s. values calculated in Eq. (3). Radial distributions were shown in Fig. 4 for water and Fig. 5 for 12.6% C.M.C.-water solution. In the turbulent core for $\phi < 0.9$, the fluctuating velocity was almost constant and almost nearly equal value of \bar{V}_z at the center. The intensities of turbulence based on the axial mean velocity at the center were 90% for axial and 50% for radial. These values were very large compared with the intensities of pipe flow (3%)⁷⁾ and that of agitated vessels (30%)⁸⁾ and would cause characteristically large axial mixing of bubble columns. Reynolds stress ($\overline{v_r v_z}$) obtained from Eq. (4) were also shown in Fig. 4 and 5 which scattered considerably.

In the bubble column, upward flow was predominant in the core and near the wall the flow moved downwards almost all the time. But even in the center, downflow sometimes occurred and near the wall, upward flow could be observed. Fig. 7 shows the ratio of upward flow time to the total time vs. radial distance. The curves were almost the same for water and C.M.C. solution and then the flow behaviour for water and for C.M.C. solution would not be different each other so much, taking account of comparison of Fig. 4 and 5. This would be consistent with the constancy of eddy diffusivity of Eq. (16) given by Miyauchi¹⁾.

The fluctuating behaviour could be observed in the wall shearing stress, too. Fig. 8 shows the fluctuating behaviour of diffusion current in the potassium ferri & ferro cyanide solution, which is proportional to the $(\tau_w)^{1/3}$. Intensity amounted to 15% for $(\tau_w)^{1/3}$.

Fig. 8 Fluctuations of diffusion current



3) Correlations of fluctuating velocity

Correlation or energy spectrum are the most important tool to analyze turbulent behaviour. Fig. 9 shows the autocorrelation coefficient curve, which is normalized from the autocorrelation function, calculated in Eq. (5) for the various radial positions. The curve for the flow near the wall ($\phi=0.92$) was noteworthy in periodic form in the range of large delay time. In order to analyze the periodicity of flow for $\phi=0.92$, the correlation was transformed to the spectrum and shown in Fig. 10 in the form of periodgram. Fig. 10 shows the peak at $f=0.65$ c/s and it is pointed out that the downward flow near the wall had characteristic periodicity of this period of time.

In the turbulent core, the violent eddies were observed moving irregularly. In order to find the scale of these eddies, the radial correlation curve was calculated from Eq. (7) and shown in Fig. 11. The curve fell to zero at the radial position of $\phi=0.77$. The integral scale, which was obtained from radial correlation by integration for $\phi=0\sim 0.77$, was 1.5 cm. This value demonstrates the existence of eddies, whose average radial diameter amounted to one sixth to one seventh of column diameter.

The area obtained by integrating the time correlation curve (Fig. 9) between $\tau=0\sim \tau_1$, in which τ_1 is the first intercept of the zero value of the correlation is called the life time of eddies. Fig. 12 shows the radial distribution of the life time. In the center,

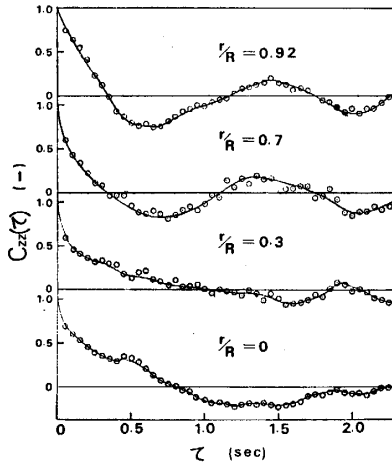


Fig. 9 Autocorrelation coefficient of time.

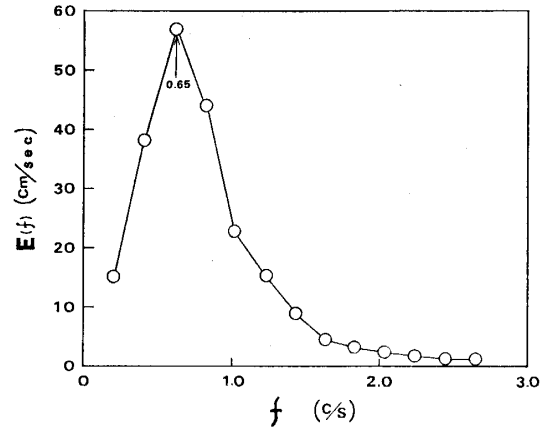
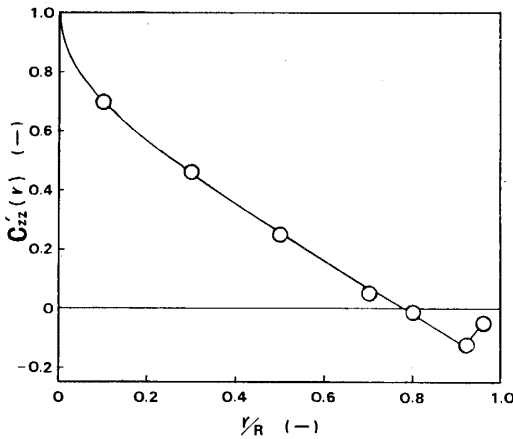
Fig. 10 Periodogram of V_z at $\phi=0.92$.

Fig. 11 Autocorrelation coefficient of radial distance.

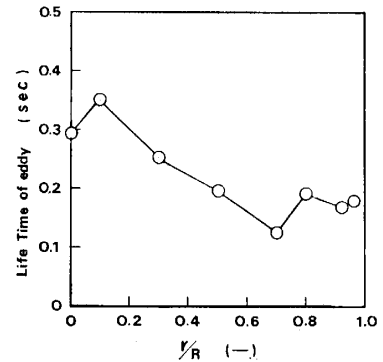


Fig. 12 Radial variation of eddy life time.

the life time amounted to 0.3 sec. The life time corresponds roughly to the integral scale of eddies by multiplying the average velocity. Then 0.3 sec of the life time at the center corresponded to the axial eddy length of about 4.2 cm. The life time behaviour seemed to be different for the region of $\phi < 0.7$ and $\phi > 0.7$, which corresponded to the radial boundary position of the up and down flow.

Conclusion

Liquid velocities in a bubble column (dia. = 10 cm ϕ) were obtained by photographing tracer particles suspended in liquid with a high speed cinecamera.

1) Average axial velocity distributions in the turbulent core were almost coincident with the circulation flow model derived by Miyauchi¹⁾ and average radial velocities were almost zero through the radial distance.

2) Intensity of turbulence was 90% of average axial velocity at the center. The r.m.s. values of axial and radial fluctuating velocity were almost constant in the turbulent

core. The flow fluctuation was violent and downward flow periods were observed even in the center.

3) The correlation of axial velocity was obtained for both time and radial distance. Radial scales were 1/6th–1/7th of column diameter and axial scales were about one half of column diameter.

4) Periodicity was observed in the downward flow region near the wall, with a period of 0.65 c/s.

5) For the viscous liquid of C.M.C. solution (12.6 c.p), the flow behaviour was almost the same as water.

Nomenclature

A	: mass transfer area of the electrode	[cm ²]
C_b	: bulk concentration of ferri-cyanide ion	[gmol/cc]
C_w	: wall concentration of ferri-cyanide ion	[gmol/cc]
D_T	: diameter of column	[cm]
D	: diffusion coefficient of ferri-cyanide ion in water	[cm ² /sec]
E	: energy spectrum	[cm ² /sec]
F	: Faraday constant	[coulomb/equiv.]
f	: frequency	[1/sec]
g	: acceleration of gravity	[cm/sec ²]
I	: diffusion limited current	[μ A]
L_e	: effective length of electrode	[cm]
R	: radius of column	[cm]
r	: radial distance	[cm]
S_x	: velocity gradient at the wall	[1/sec]
t	: time	[sec]
u^+	: dimensionless velocity ($V_z/\sqrt{\tau_w/\rho}$)	[—]
U_g	: superficial velocity of gas	[cm/sec]
V_r	: radial velocity	[cm/sec]
V_z	: axial velocity	[cm/sec]
v_r	: fluctuating radial velocity	[cm/sec]
v_z	: fluctuating axial velocity	[cm/sec]
y	: distance from the wall	[cm]
y^+	: dimensionless distance of y ($y\rho\sqrt{\tau_w/\rho}/\mu$)	[—]
z	: axial distance	[cm]
ε_0	: gas hold-up at the center	[—]
ρ	: liquid density	[g/cm ³]
μ	: viscosity of liquid	[g/cmsec]
μ_t	: eddy viscosity	[g/cmsec]
ϕ	: r/R	[—]
τ_w	: shearing stress at the wall	[Gr/cm ²]
τ	: delay time of autocorrelation	[sec]

References

- 1) Miyauchi, T and C. N. Shyu: "Flow of fluid in gas-bubble columns" Chem. Eng. (Japan) 34 (9) 50-56 (1970) (in Japanese)
- 2) Yoshitome, H and T, Shirai: "The intensity of bulk flow in a bubble bed" J. Chem. Eng. Japan 3 (1), 29-33 (1970) (in Japanese)
- 3) Koide, K and H, Kubota: "Gas holdup distribution and liquid velocity distribution on bubble flow in vertical column" Chem. Eng. (Japan) 30 (9) 50-57 (1966) (in Japanese)
- 4) Kojima, E, T, Akehata and T, Shirai: "Turbulence of liquid flow in bubble columns with one hole nozzle" Preprint of 11th Chem. Engrs. Symposium at Kyoto (1973) 39-44 (in Japanese)
- 5) Akaike, H: Annals Inst. Statistical Math. 14, 1 (1962)
- 6) Hanratty, T. J. and P. V, Shaw: "Fluctuation in the local rate of turbulent mass transfer to a pipe wall" A.I.Ch.E. Journal 10 (4), 475-482 (1964)
- 7) Hinze, J. O: "turbulence" McGraw-Hill (N.Y.) p 521 (1959)
- 8) Sato, Y and K, Yamamoto et al: Chem. Eng. (Japan) 31 (3) 279 (1967) (in Japanese)